Cement and Concrete Research 40 (2010) 1571–1581

Contents lists available at ScienceDirect

Cement and Concrete Research

journal homepage: http://ees.elsevier.com/CEMCON/default.asp

Behaviour of Slurry Infiltrated Fibre Concrete (SIFCON) under triaxial compression

Y. Farnam [a,*], M. Moosavi [b], M. Shekarchi [a], S.K. Babanajad [a], A. Bagherzadeh [a]

[a] Construction Materials Institute, School of Civil Engineering, College of Engineering, University of Tehran, Tehran, Iran
[b] School of Mining Engineering, College of Engineering, University of Tehran, Tehran, Iran

ARTICLE INFO

Article history:
Received 12 January 2010
Accepted 25 June 2010

Keywords:
Triaxial strength
Confining pressure
Steel fibre
SIFCON
Failure criterion

ABSTRACT

Slurry infiltrated fibre concrete (SIFCON) is one of the recently developed construction material that can be considered as a special type of high performance fibre reinforced concrete (HPFRC) with higher fibre content. In the current research, triaxial compressive behaviours of high strength concrete (HSC), HPFRC and SIFCON were investigated. Purposefully, laboratory tests employed on four types of 75×150 mm cylindrical specimens with different steel fibres volumes (0, 2, 5 and 10%). All tests were conducted under four different confining pressure levels (0, 5, 15 and 21.5 MPa) according to triaxial conditions. Consequently, stress-strain curves were obtained and governing failure patterns and failure criterions of HSC, HPFRC and SIFCON samples were discussed. According to the results increasing of fibre volumes increases peak stress, energy absorption, toughness and Poisson's ratio while increasing confining pressures increases peak stress, energy absorption and toughness. Also, this may cause concrete to behave as a plastic material.

1. Introduction

Development of modern civil engineering causes an urgent need to develop higher performance engineering materials possessing high strength, toughness, energy absorption and durability. Fibre reinforced concrete (FRC) is one of the conventional engineering materials used in several structural applications in order to enhance the structural resistance/performance under different loading combinations. It also increases speed of construction and may even eliminate the need for conventional reinforcement. High or ultra-high strength concrete with very high compressive strength values remains basically a brittle material. The inclusion of adequate fibres improves tensile strength and provides ductility [1–4].

While the fibre volume fraction of conventional fibre reinforced concrete and high performance fibre reinforced concrete (HPFRC) is generally limited to 1–3%, some special composites are produced with fibre volume fraction values between 3% and 20% [5,6]. These composites can be classified as SIFCON (slurry infiltrated fibre concrete), which has high ductility and tensile strength properties with high strength cementitious matrix. The mechanical properties of SIFCON have been investigated widely and it is found that SIFCON can provide several times higher strength than that of the matrix. It can also increase the flexural toughness even more [7,8]. Due to the interlocking effect of high volume of steel fibres, making SIFCON with ordinary mixing procedures is not possible. Solving this problem, the fibres are preplaced in the formwork moulds to its full capacity. Then resulting fibre network is infiltrated by cement based slurry. Infiltration is usually accomplished by gravity flow together with light vibration or by pressure grouting [7].

According to the literature review, it has been realized that although there are many studies on the triaxial behaviour of normal concrete, high strength concrete (HSC), and high strength fibre reinforced concrete (HSFRC) [9–18], no comprehensive studies have been conducted on the triaxial behaviour of SIFCON. The obtained results from triaxial behaviour can be employed in several applications like design of various types of concrete element/structures such as plates, shells, pre-stressed concrete, pressure vessels, marine structures, underground structures and other types of containment structures. It can also be used to the structural design of elements subjected to lateral forces like wind and earthquake.

Linhua et al. [9] carried out a series of triaxial tests on normal strength concrete by a special device applying two lateral compressive and one longitudinal tensile loads in three dimensions. They studied stress-strain relationships and failure modes of the samples. Chern et al. [10] studied the response of FRC subjected to multiaxial loading conditions. They performed uniaxial compression tests, split cylinder tests (to acquire tensile properties) and a series of triaxial tests that included various loading paths. Xie et al. [11] conducted a series of triaxial tests on HSC samples under confining pressure. The compressive strength of samples ranged from 60.2 to 119 MPa. Their triaxial tests involved 55.5×110 mm cylindrical samples. In their experiments, confining pressures (σ_3) and confinement ratios (σ_3/f'_c, where f'_c is uniaxial compressive strength) ranged from 11.9 to 59.97 MPa and 0.1 to 0.504 respectively. In a similar manner, Attard and Setunge [12] performed a series of triaxial tests on larger cylindrical samples (100×200 mm) involving concretes with

* Corresponding author. Tel.: +98 912 6134164.
E-mail address: yfarnam@ut.ac.ir (Y. Farnam).

0008-8846/$ – see front matter © 2010 Elsevier Ltd. All rights reserved.
doi:10.1016/j.cemconres.2010.06.009

strengths as high as 109 MPa. Their experiments were performed at low confining pressure levels with a maximum confinement ratio of 0.16. Imran and Pantazopoulou [13] studied the behaviour of plain concrete under triaxial stress state and the damage characteristics of concrete under dry and saturated conditions. Ansari and Li [14] performed a series of triaxial tests on 100×200 mm cylindrical samples involving concretes with strengths as high as 103 MPa. Their experiments were performed at very high confining pressure levels with a maximum confinement ratio of 1.0. Li and Ansari [15] investigated on the effect of specimen size for very high strength concrete under triaxial test subjected to very high confining pressure. They indicated that there is a slight size effect on the failure strength of HSC in triaxial compression.

Mahboubi and Ajorloo [16] carried out an extensive experimental parametric study on the mechanical responses of various types of plastic concrete in uniaxial and triaxial compression tests. They investigated on the effect of specimen age, cement factor, Bentonite content and confining pressure on shear strength and permeability of plastic concrete. Lu and Hsu [17] studied on the behaviour of HSC and HSFRC (with 1.0% volume ratio of steel fibre) under uniaxial and triaxial compression. They also investigated on triaxial stress–strain relations and failure criteria. They indicated that low volume ratio of steel fibre reinforcement has an insignificant effect on the nonlinear stress–strain relation of HSC under the triaxial compression. Candappa et al. [18] performed a series of triaxial tests under low confining pressures on the four high-strength concretes with uniaxial compressive strengths of 41.9 to 103.3 MPa. They also calibrated two failure criterions with related experimental data. Grigin et al. [19] gathered a comprehensive collection of triaxial test data and empirical relationships in literature. They also suggested analytically a relationship to predict the ultimate strength of very high strength concrete under triaxial compression and compared it to the data taken from literature.

Review of technical literature indicates that there are not any exhaustive available data regarding the response of SIFCON and HSC with notable variety of steel fibres content subjected to triaxial compression. The experimental program includes a wide range of experiments in which two types of SIFCON are compared with HSC and HPFRC under different confining pressures up to 21.5 MPa. Subsequently, the effect of fibre content and level of confining pressure on the stress-strain responses, mechanical properties of specimens, energy absorption capacity (toughness), failure patterns, and failure criterions are discussed.

2. Experimental Program

Three types of concrete were used in the current study, namely high strength concrete (HSC), high performance fibre reinforced concrete (HPFRC) and Slurry infiltrated fibre concrete (SIFCON). Also, four different steel fibre volume fractions (V_f) have been employed (0, 2, 5 and 10%). The classes of samples are therefore HSC (V_f=0%), HPFRC (V_f=2%), SIFCON5 (V_f=5%) and SIFCON10 (V_f=10%). During the experimental program, only one type of matrix was used for all samples.

Cementitious materials were ordinary Portland cement (OPC), in accordance with ASTM Type II, and silica fume as a pozzolan additive. The chemical analyses of materials are given in Table 1. The aggregates were crushed limestone with maximum size of 1 mm. These fine aggregates had specific gravity and absorption values of 2.50 and 3.2%, respectively. The water-cementitious material ratio (w/cm) of the mixture was 0.33. Moreover, highly effective polycarboxylate chemical additive was used as a superplasticizer to provide fluidity and workability of the mixture. The amounts of polycarboxylate used in the tests are 1.3% mass of cementitious material for HPFRC and HSC and 1.5% mass of cementitious material for SIFCON5 and SIFCON10. The mortar mix proportions are listed in Table 2. Also, the properties of straight smooth steel fibre employed in the mortar are presented in Table 3.

Table 1
Chemical analyses of ordinary Portland cement and silica fume.

Chemical analyses, %	Cement	Silica fume
Silicon dioxide (SiO_2)	21.03	93.16
Aluminium oxide (Al_2O_3)	4.53	1.13
Ferric oxide (Fe_2O_3)	3.63	0.72
Calcium oxide (CaO)	62.45	-
Magnesium oxide (MgO)	3.42	1.6
Sodium oxide (Na_2O)	0.21	-
Potassium oxide (K_2O)	0.55	-
Sulphur trioxide (SO_3)	2.23	0.05
Loss on ignition (LOI)	1.37	1.58

In order to prepare specimens, cement, silica fume and aggregates were first blended together in a dry condition. Then, water was mixed with superplasticizer and gradually was added to the cement mixture to provide a homogeneous mortar, categorized as a self-consolidation concrete (SCC). The prepared mortar was then poured into 75×150 mm cylindrical steel moulds in several layers. After pouring each layer, fibres were randomly dispersed in a horizontal direction. Furthermore, soft vibration was applied to SIFCON samples to make sure that the matrix completely surrounds the fibres. For SIFCON, some more superplasticizer samples were used to create more flowable mortar to facilitate easy-penetration into high content of fibres [20].

Freshly cast specimens were then kept in the mould for 24 hours: afterwards, they were demoulded and stored in water. The water was saturated with calcium hydroxide at 22 °C and samples were remained there for 90 days. Then, the specimens were taken out of the curing room and were carefully capped at both ends to provide flat and smooth bearing areas for the loading platens.

3. Testing Procedure

32 samples with four different steel fibre contents (0, 2, 5 and 10% by volume) were tested in triaxial compression under confining pressure up to 21.5 MPa. Among all conducted tests, maximum confinement ratio (σ_3/f'_c) was approximately 0.3. Designations of triaxial compression tests are listed in Table 4.

Cylindrical specimens with diameter and height of 75×150 mm were prepared in order to carry out triaxial tests. In accordance with ASTM C801 [21], a triaxial Hoek cell [22] was used to determine the behaviour of specimens under confined lateral conditions.

The load path for triaxial tests is given in Fig. 1. As shown, equal values of axial and confining pressures were simultaneously applied to the specimens until the confining pressures (hydrostatic pressure, σ_3) reached the definite value. At this point, the confining pressure was kept constant and the additional axial stress ($\Delta\sigma$) was increased at a constant strain rate of 0.0001 per second through the platens located at its ends. A rubber bladder was utilized to isolate the specimen from oil penetration.

All triaxial tests were performed by the MTS machine (Fig. 2), with a rigid frame and capacity of 4500 KN. The axial actuator and confining

Table 2
Mortar mix proportion.

	Type	kg/m³
Cement	Portland (Type II)	1000
Pozzolan	Silica fume	175
Aggregate	Sand (0-1 mm)	835
Water	-	388
w/cm	-	0.33
Superplasticizer	Polycarboxylate (Gleniume)	15.3-17.6 (1.3-1.5% of cementitious material by mass)

Table 3
The properties of straight smooth steel fibre.

Fibre type	Steel fibre
Section shape	Circle
Length (mm)	30
Diameter (mm)	0.25
l/d (aspect ratio)	120
Tensile strength (MPa)	2200

pressure intensifier were programmed together to provide the desired load paths. During the tests, load and deformation data was recorded and stored by the data acquisition system and subsequently was processed for analysis. A confining pressure intensifier was used to fill and pressurize the triaxial cell with confining fluid. The confining pressure σ_3 is directly measured by a pressure transducer.

Increasing the additional axial stress causes the specimen to dilate (or contract) in the triaxial cell. In order to keep the lateral confining pressure constant, some oil should be drained out of (or inject into) the cell. To do this, an external hydraulic pressure controller equipped by a jack was used. In other words, in response to the specimen dilation (or contraction) in the cell, the jack was relaxed (or compressed) to accommodate a volume of oil which is equal to the specimen's volume change. Therefore, oil transmitted from the cell to the jack (and vice versa) during the test to guarantee constant load in the jack and consequently constant pressure in the cell. This arrangement kept confining pressure constant with 0.5% accuracy. Also, the volume changes associated with the movement of the jack were measured by using LVDT.

In order to measure axial and lateral strains accurately, adequate calibration tests were performed. First, platen movement of the pressing machine and volume changes were calibrated using high accuracy strain gauges with 10^{-5} mm/mm reading. Then, the recorded strain measurements for the rest of the tests were calibrated.

4. Result and Discussion

4.1. Stress-strain responses under triaxial compression

In order to obtain additional axial stress-strain and volumetric strain-strain curves, two samples were tested and the results were averaged as shown in Fig. 3. In all curves, contraction and dilation are designated as positive and negative, respectively.

4.1.1. Effect of confining pressure

The experimental responses of HSC, HPFRC, SIFCON5 and SIFCON10 specimens under different confining pressures are plotted

Table 4
Designation of triaxial compression tests.

Designation (Fibre volume ratio)	Specimen designation	Confining pressure (MPa)	Confinement ratio (σ_3/f'_c)
HSC ($V_f=0\%$)	HSC-0	0	0
	HSC-5	5	0.06
	HSC-15	15	0.20
	HSC-21.5	21.5	0.29
HPFRC ($V_f=2\%$)	HPF-0	0	0
	HPF-5	5	0.06
	HPF-15	15	0.17
	HPF-21.5	21.5	0.25
SIFCON5 ($V_f=5\%$)	SIF5-0	0	0
	SIF5-5	5	0.04
	SIF5-15	15	0.11
	SIF5-21.5	21.5	0.15
SIFCON10 ($V_f=10\%$)	SIF10-0	0	0
	SIF10-5	5	0.03
	SIF10-15	15	0.09
	SIF10-21.5	21.5	0.13

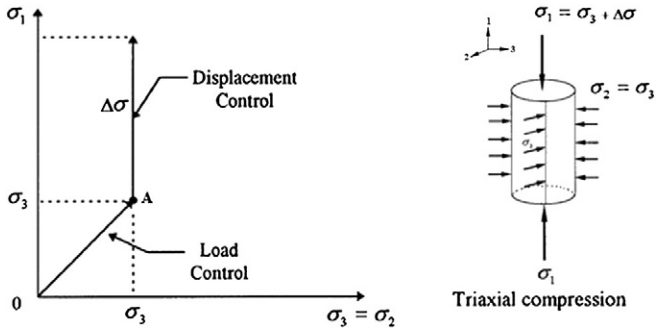

Fig. 1. Loading path for triaxial tests.

in Figs. 4–7, respectively. It is obvious that by increasing confining pressure at a constant content of steel fibres, additional axial stress and triaxial compressive strength were increased. Concrete samples behave as a ductile and plastic material in the presence of confining pressure. This characteristic is observed particularly in the HSC and HPFRC samples, while ductile behaviour is inherent in the SIFCON samples because of high content of steel fibres.

Three types of relationship can be observed between the evolution of the volumetric strain history and characteristics of compressive stress-strain curve in the plots due to the three types of material behaviour. These behaviours are softening, plastic and hardening behaviour shown in Fig. 8. It should be noted that in ideally elastic conditions, ε_v (volumetric strain) is defined by ε_a-$2\varepsilon_l$ formula where ε_a and ε_l are absolute values of axial strain and lateral strain under triaxial compressive test, respectively. At point ε_{a1} (end of elastic behaviour) the additional axial stress-axial strain curve deviates from linearity and specimens are contracted at a lower rate than the elastic stage because of the initiation of some micro-cracks.

In softening behaviour, the generation of multiple cracks cause the volumetric-axial strains relationship eventually to become expansive beyond the point ε_{a2} in the axis of axial strains. The descending branch of stress-strain curve is associated with this phase of volumetric growth and at point ε_{a3} contraction of specimen changes to expansion.

During applying axial load in the triaxial tests, specimen contracts in axial direction while dilation occurs in the lateral direction due to Poisson's law. There are two parameters controlling lateral dilation, namely confining pressure and fibre content. Also, both of them control the development of cracks which cause specimen to dilate faster.

According to stress-strain responses for HSC specimens (Fig. 4), softening behaviour was observed in the samples for all confining

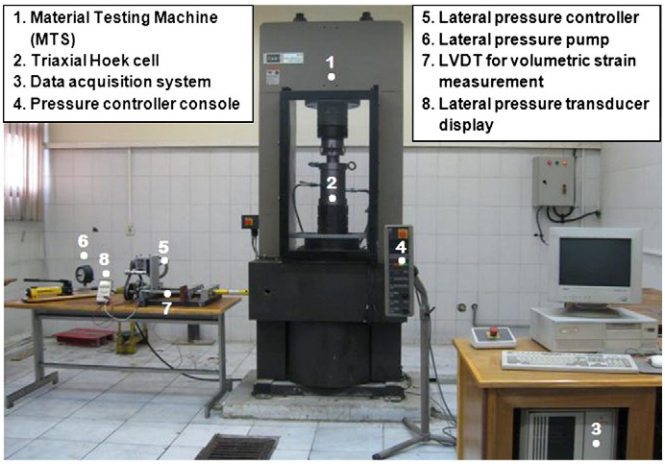

Fig. 2. Triaxial test setup.

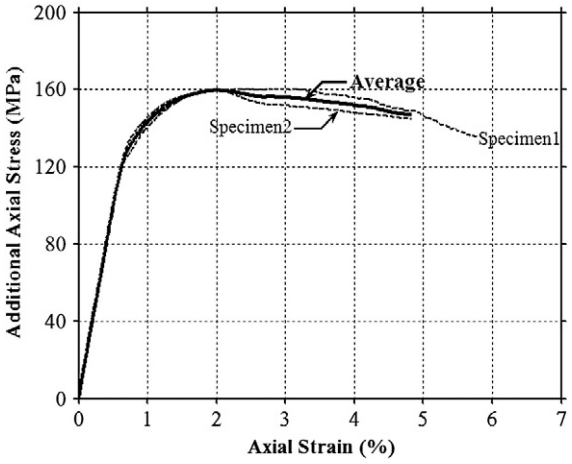

Fig. 3. The process of calculating average of two stress-strain curves for HPF-21.5 specimens as an example.

pressures (0 to 21.5 MPa). This behaviour is manifested by a drop in peak load and then residual strength is reached. However, at higher confining pressures (15 and 21.5 MPa), due to the less crack developments, the samples showed more plastic behaviour and the volumetric strain curves remained in the contraction region. The flat response of the volumetric change section after the peak load can be mainly attributed to the frictional movement of two collapsed parts which doesn't cause any volumetric strain in the specimens (Fig. 9). In other words, after the drop, the procedure of triaxial test may be changed towards shear test condition. This phenomenon was visually observed on the samples taken away from the cell with notable distinct shear plane.

As shown in Fig. 5, adding fibre to HPFRC may lead to a more ductile behaviour in the specimens. This behaviour is very notable in the specimens under uniaxial compression test (without confining pressure). Also, the peak point moves towards right (higher axial strains) as the confining pressure increases. For specimens under 0 and 5 MPa confining pressure, softening behaviour was observed which attributed to more crack development. As the cracking develops, the volumetric strain changes from contraction to dilation

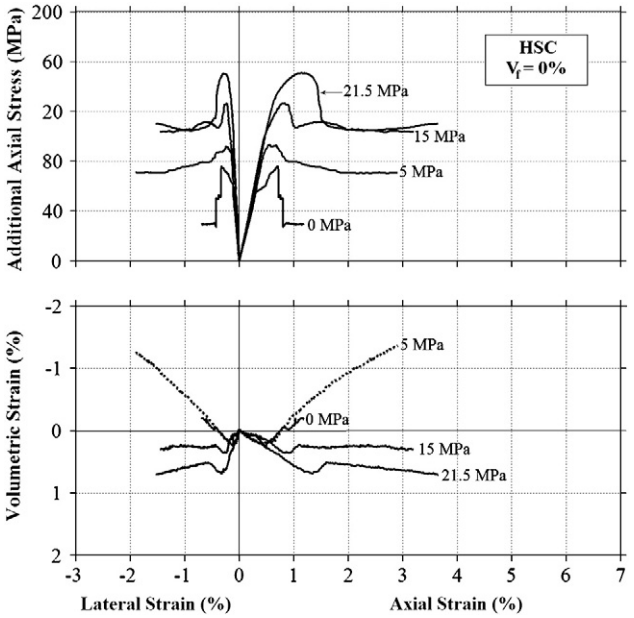

Fig. 4. Additional axial stress and volumetric strain versus strain for HSC samples under triaxial testing conditions.

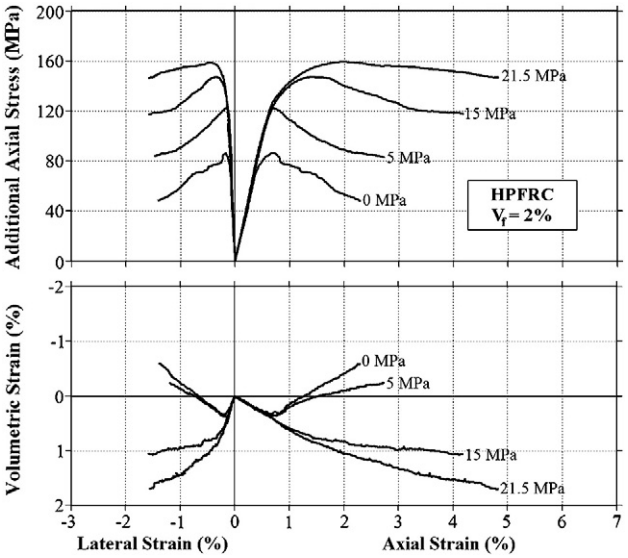

Fig. 5. Additional axial stress and volumetric strain versus strain for HPFRC samples under triaxial testing conditions.

mode. Therefore, adding steel fibre seems not to be sufficient to prevent crack propagation and lateral expansion. However, for higher confining pressures the crack development is not so pronounced and the samples deform more as a plastic material. Hence the samples cannot recover their contraction.

SIFCON showed a distinguished performance to control cracking because of high volume fractions and appropriate orientation of steel fibre. Studying on the SIFCON stress-strain response (Figs. 6 and 7) indicates that adding steel fibre may properly control the crack propagation and lateral expansion during axial loading. This has caused SIFCON to indicate hardening behaviour at all confining pressure levels under triaxial loading and it has also increased the peak triaxial compressive strength. However, this increase is not a linear function of confining pressure and it becomes less significant as the confining pressure reaches over 15 MPa. It should be noted that this effect is more pronounced for SIFCON10. In other words, 5% steel fibre is enough to provide sufficient confinements to inhibit major

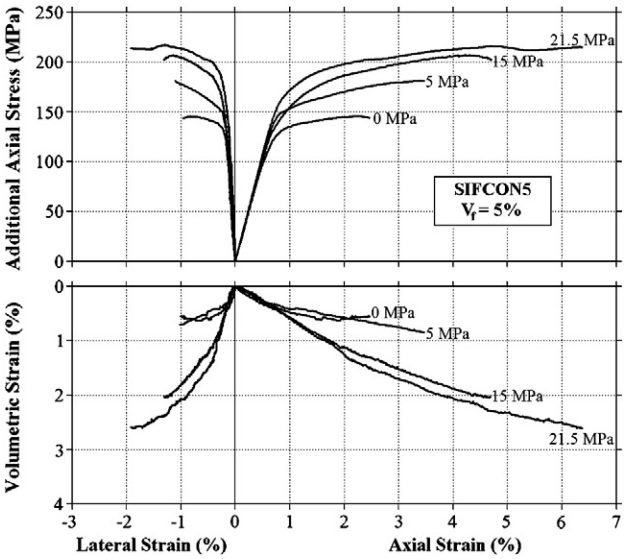

Fig. 6. Additional axial stress and volumetric strain versus strain for SIFCON5 samples under triaxial testing conditions.

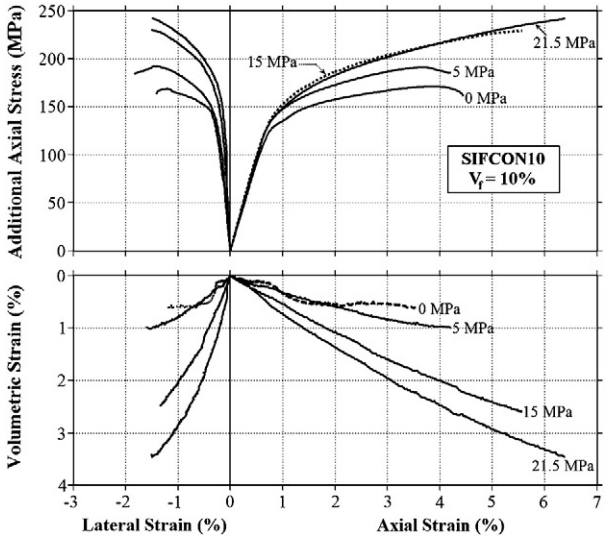

Fig. 7. Additional axial stress and volumetric strain versus strain for SIFCON10 samples under triaxial testing conditions.

crack growth. Only for SIFCON5 with no confining pressure a rather softening behaviour was observed.

Comparison between stress-strain responses of HSC, HPFRC, SIFCON5 and SIFCON10 under different confining pressures revealed that with the increase of fibre volume content, the dependency of triaxial mechanical behaviour to the value of confining pressure is decreased. This fact is remarkable particularly for SIFCON samples

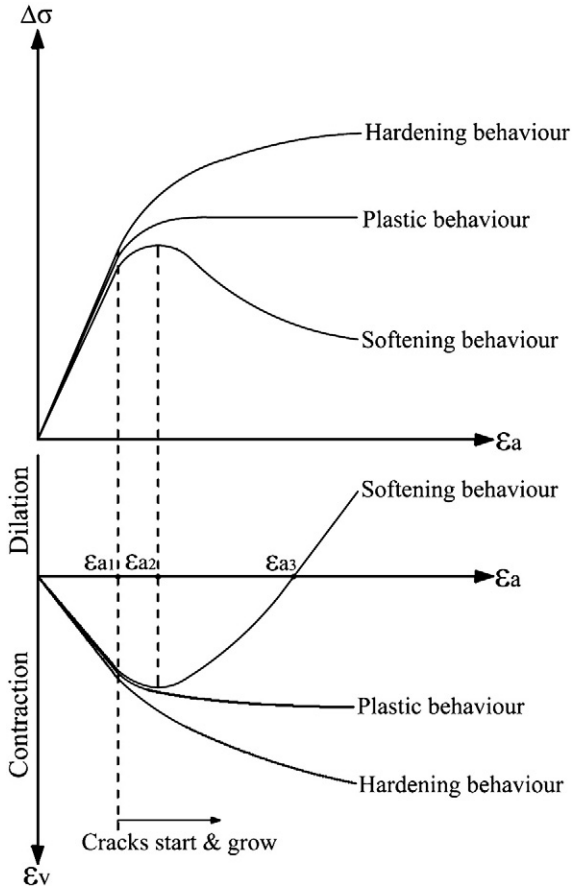

Fig. 8. The schematic of volumetric strain and additional axial stress versus axial strain.

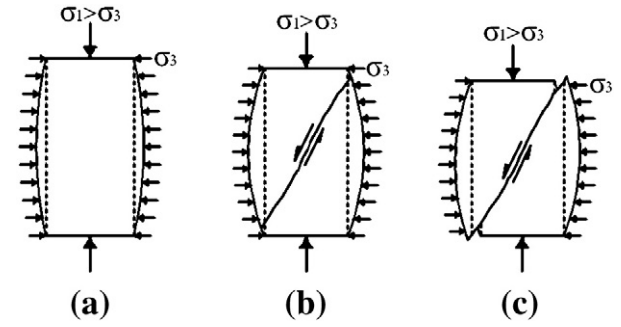

Fig. 9. Shear failure for HSC specimens under triaxial compression test: (a) before shear cracking; (b) the moment of occurring shear cracks; and (c) relative frictional movement of two shear parts which doesn't cause any volumetric variation.

where increasing the confining pressure from 15 to 21.5 MPa did not result in notable difference in the strength.

4.1.2. Effect of fibre volume fraction

In Figs. 10–13, the experimental responses of all four types of specimens with different steel fibres volume fraction under 0, 5, 15 and 21.5 MPa confining pressure are plotted, respectively. As shown in these figures, by increasing steel fibre content in a constant confining pressure condition, the plastic behaviour and total strength increase and the samples tend to dilate less. Depending on the confining pressure, it seems that a transition from softening to plastic behaviour can be predicted between 2-4% fibre content.

It is remarkable that except for samples loaded uniaxially, adding steel fibre up to 5% has considerable effect on increasing triaxial compressive strength. Consequently, 5% of fibres content is adequate to control sample expansion and crack propagation under triaxial loading and adding more fibre has small effects.

4.2. Mechanical properties

Mechanical properties of HSC, HPFRC and SIFCONs under triaxial compression are summarized in Table 5. Considering uniaxial test, the peak uniaxial compressive strengths in 2, 5 and 10% steel fibres samples are 1.14, 1.92 and 2.25 times larger than HSC samples, respectively. Moreover, the ratios of the peak additional axial stress under 21.5 MPa for HSC, HPFRC, SIFCON5 and SIFCON10 in relation to

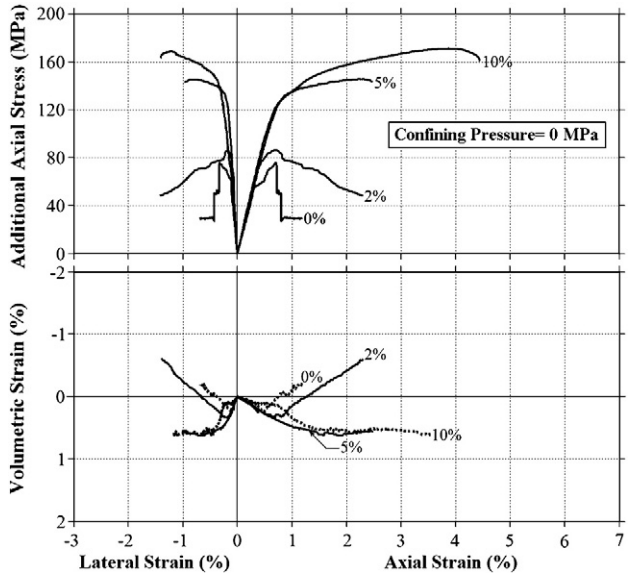

Fig. 10. Additional axial stress and volumetric strain versus strain for samples with different steel fibre volume fraction under uniaxial compressive test.

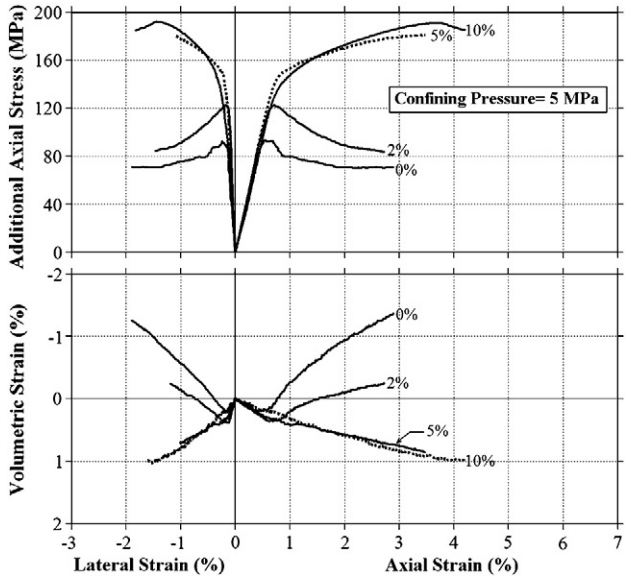

Fig. 11. Additional axial stress and volumetric strain versus strain for samples with different steel fibre volume fraction under 5 MPa triaxial confining pressures.

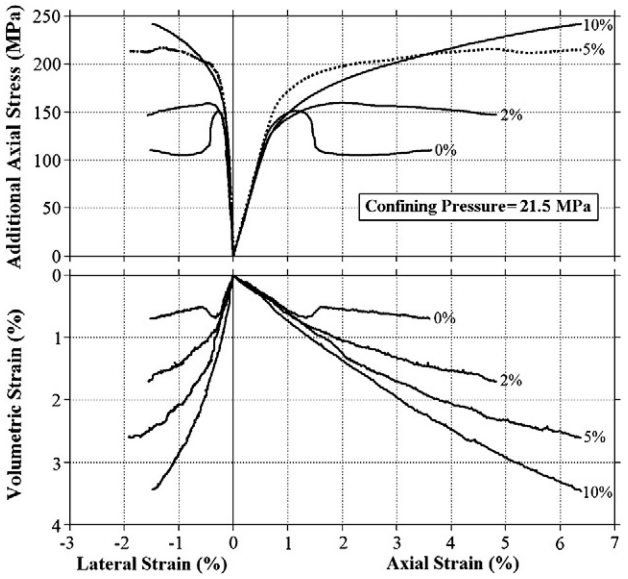

Fig. 13. Additional axial stress and volumetric strain versus strain for samples with different steel fibre volume fraction under 21.5 MPa triaxial confining pressures.

samples with no confining pressure are 1.99, 1.84, 1.48, and 1.42, respectively. It seems that the effectiveness of increasing confinement pressure on the strength of samples will decrease when the volume fraction of steel fibres increases.

Peak additional axial stress versus confining pressure for HSC, HPFRC and SIFCONs are plotted in Fig. 14. Note that the maximum additional axial stress observed during the triaxial tests on each specimen was recorded as the peak additional axial stress. As illustrated in this figure, increase of both confining pressure and fibre content resulted in upper peak additional axial stress. Considering nonlinear increasing trend of HPFRC and SIFCON specimens up to 21.5 MPa confining pressure, it seems that HSC have a linear trend based on the number of performed tests. In addition, from comparing graphs in Fig. 14 it is remarkable that for samples which are containing fibre volume less than 5%, fibre volume has a dominant effect in increasing strength. This enhancement decelerates from 5 to 10% of steel fibre.

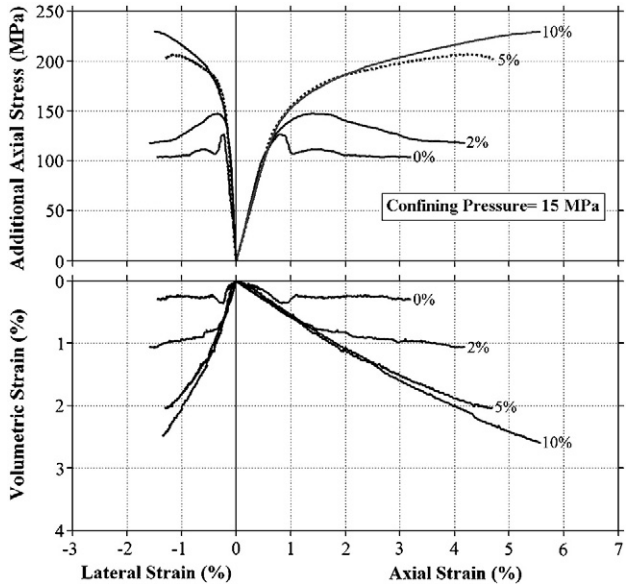

Fig. 12. Additional axial stress and volumetric strain versus strain for samples with different steel fibre volume fraction under 15 MPa triaxial confining pressures.

Variations of Poisson's ratio (ν) for HSC, HPFRC and SIFCON under 0, 5, 15 and 21.5 MPa confining pressure are presented in Fig. 15. It should be noted that obtained Poisson's ratio is calculated by dividing the slope of additional axial stress-axial strain curve by the slope of additional axial stress-lateral strain curve in the limit of linearity which is equal to $\nu_{12}=\nu_{13}$ (for definition of local axes see Fig. 1). According to Fig. 15, the maximum and minimum values of Poisson's ratio match to SIFCON10 and HSC samples, respectively. In other words, by increasing the steel fibre content, Poisson's ratio increases. Moreover, due to high amounts of steel fibre in the direction of 2-3 plane, SIFCONs may behave like a transversely isotropic material, whose properties in two directions are different. Here, only ν_{12} or ν_{13} were measured according to applied loading procedure and test setup.

4.3. Energy absorption capacity (toughness)

The area under the stress-strain curve is a measure of toughness of the material. Researchers have used different definitions for the toughness using the area under the curve. Fanella and Naaman [23] have defined the toughness of FRC as the ratio of toughness of the

Table 5
Mechanical properties of HSC, HPFRC and SIFCONs under triaxial compression.

Specimen	Confining pressure (MPa)	Modulus of elasticity, E (GPa)	Poisson's ratio (ν)	Peak additional axial stress (MPa)	Relative peak additional axial stress [a]
HSC ($V_f=0\%$)	0	17.3	0.20	76	1.00
	5	19.9	0.22	93	1.22
	15	21.4	0.21	126	1.66
	21.5	20.9	0.19	151	1.99
HPFRC	0	18.7	0.23	87	1.14
($V_f=2\%$)	5	20.5	0.20	123	1.62
	15	20.0	0.21	147	1.93
	21.5	19.9	0.21	160	2.11
SIFCON5	0	20.2	0.24	146	1.92
($V_f=5\%$)	5	20.9	0.24	181	2.38
	15	21.2	0.26	207	2.72
	21.5	22.1	0.23	216	2.84
SIFCON10	0	18.2	0.29	171	2.25
($V_f=10\%$)	5	18.5	0.28	191	2.51
	15	20.9	0.26	229	3.01
	21.5	19.8	0.25	242	3.18

[a] Ratios of the peak additional axial stress to that of HSC with no confining pressure.

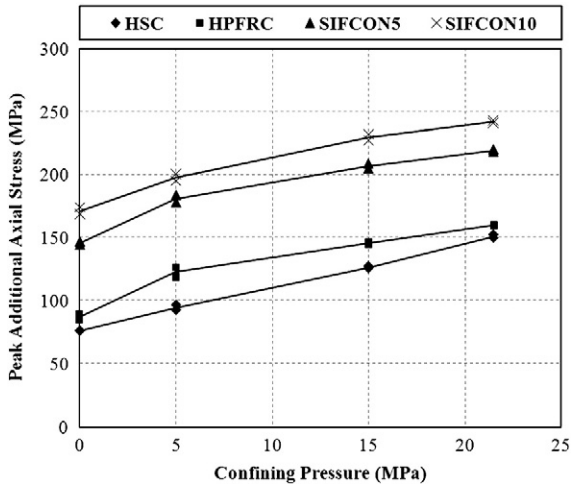

Fig. 14. Peak additional axial stress versus confining pressure for HSC, HPFRC and SIFCONs.

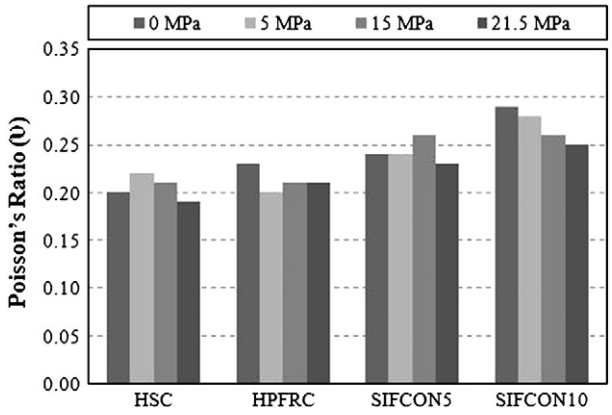

Fig. 15. Poisson's ratio for HSC, HPFRC and SIFCONs under different confining pressure.

fibre reinforced matrix to that of the unreinforced control matrix. Here, this ratio is greater than unity. It can also be defined as the ratio of area of the descending part, to the area of the ascending part of the stress-strain curve. Nataraja et al. [3] have defined a toughness ratio (TR) by comparing the calculated toughness to the toughness of a rigid plastic material. In this form, the calculated ratio is less than unity for normal strength FRC.

Most researchers [3,23,24] have obtained the energy absorption capacity or toughness of FRC in compression as the area under the stress–strain curve calculated up to a specified strain value near the strain of 0.015, though the specimens still had significant resistance left. According to the results obtained in current research, HPFRC and especially SIFCONs under triaxial loading indicated totally different behaviour rather than normal FRC. In some cases, hardening behaviour was observed and the stress-strain response had entirely ascending trend and no descending trend was observed. These show high energy capacity of SIFCONs under uniaxial and triaxial compressive loadings. Therefore, in this paper in order to define a convenient method for calculating toughness of HPFRC and SIFCONs under triaxial loading, a similar way corresponding to ASTM C1018 [25] for calculating flexural toughness and first-crack strength of FRC was adopted.

The suggested method was used for the determination of a ratio named toughness index (TI) that identify the energy absorption capability of material up to the selected strain criteria in comparison to control material (i.e. material with no fibre and no confining pressure). This index is determined by dividing the energy absorption of specimen up to a specified strain criterion, by the energy absorption of HSC with no confining pressure up to the strain at which first crack is deemed to have occurred. To calculate energy absorption, energy of all three directions is considered with the following equation:

$$\textit{Energy Absorption per volume unit}\,(EA) = \int \sigma_a . d\varepsilon_a - 2\int \sigma_3 . d\varepsilon_l \qquad (1)$$

where σ_a, ε_a, σ_3 and ε_l are absolute values of additional axial stress, axial strain, confining pressure and lateral strain respectively, and $\int \sigma_a . d\varepsilon_a$ is the area under the additional axial stress-axial strain curve.

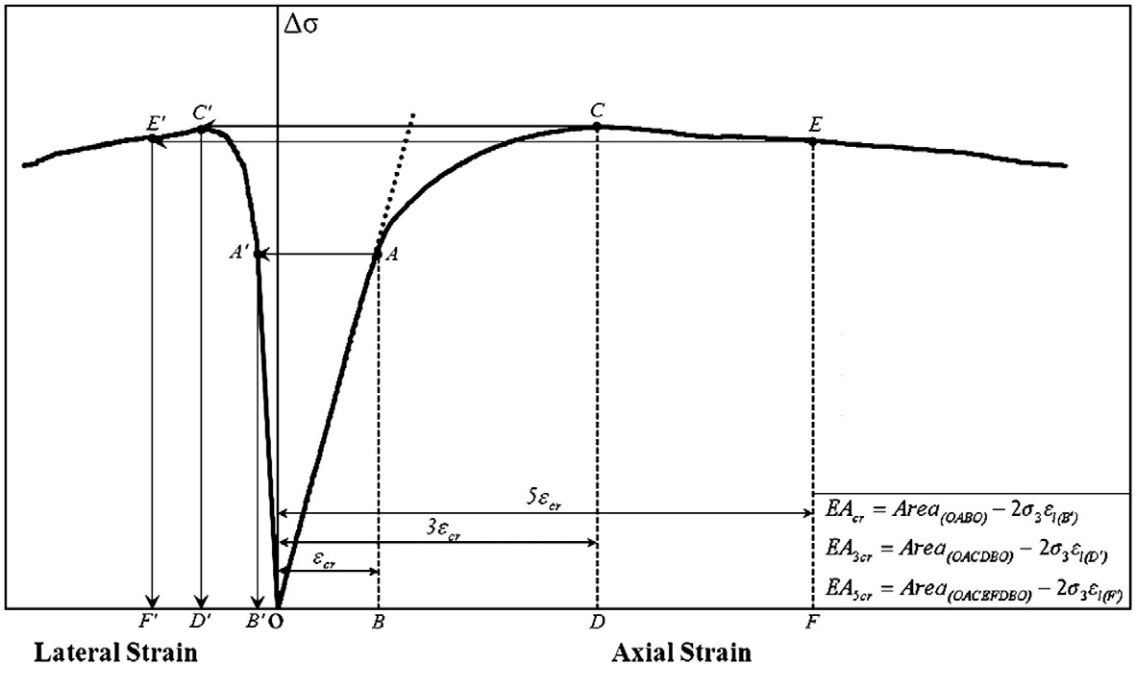

Fig. 16. Definition of parameter for calculating toughness indices in terms of multiples of first-crack deflection.

Table 6
Toughness indices of HSC, HPFRC and SIFCONs under triaxial compression.

Specimen	Confining pressure (MPa)	ε_{cr} (%)	TI_1	TI_3	TI_5
HSC (V_f=0%)	0	0.30	1.0	-	-
	5	0.41	1.9	10.0	17.1
	15	0.46	2.4	14.6	25.7
	21.5	0.65	4.8	23.6	38.2
HPFRC (V_f=2%)	0	0.36	1.5	8.9	15.3
	5	0.55	3.9	18.5	30.1
	15	0.65	4.8	27.0	46.9
	21.5	0.64	4.6	27.2	51.1
SIFCON5 (V_f=5%)	0	0.56	4.1	23.6	-
	5	0.65	5.5	31.6	60.8
	15	0.69	5.6	34.3	67.5
	21.5	0.74	6.7	40.8	77.8
SIFCON10 (V_f=10%)	0	0.71	5.9	32.5	62.9
	5	0.68	5.4	32.6	64.1
	15	0.72	5.9	35.7	71.5
	21.5	0.73	6.1	36.0	72.0

Because confining pressure is constant, therefore Eq. (1) can be summarized as:

$$EA = \int \sigma_a . d\varepsilon_a - 2 \times (\sigma_3) \times \varepsilon_l \tag{2}$$

In current paper, three toughness indices were calculated for each triaxial test: TI_1, TI_3, and TI_5 which are determined by:

$$TI_1 = \frac{EA_{cr}}{EA_{cr_0}} \tag{3}$$

$$TI_3 = \frac{EA_{3cr}}{EA_{cr_0}} \tag{4}$$

$$TI_5 = \frac{EA_{5cr}}{EA_{cr_0}} \tag{5}$$

where EA_{cr}, EA_{3cr}, and EA_{5cr} are the energy absorptions up to the corresponding first-crack strain (ε_{cr}), three times of ε_{cr}, and five times of ε_{cr} respectively, and EA_{cr_0} is the energy absorption for HSC with no confining pressure up to the first-crack strain, see Fig. 16. As shown in Fig. 16, first-crack strain (ε_{cr}) is calculated from the additional axial stress-axial strain curve where is deemed that the elastic behaviour ends and changes to nonlinearity (ε_{cr} is equal to ε_{a1} in Fig. 8). By this approach, the toughness of the material can be easily evaluated and the results are presented in the Table 6. Here, EA_{cr_0} is equal to 0.0772 (MPa.mm)/mm. The variation in the toughness indices is between 1 and 78. The highest toughness is obtained by SIFCON5 under 21.5 MPa confining pressure. Both confining pressure and fibre content have good effect on the toughness indices.

4.4. Interrelated effects of fibre volume fraction and confining pressure

For better description of interrelated effects of fibre volume fraction and confining pressure, five ratios, namedR_{TI_1}, R_{TI_3}, R_{TI_5}, $R_{\Delta\sigma_{peak}}$ and $R_{\varepsilon_{cr}}$, are defined as:

$$R_{TI_1} = \frac{(TI_1)_{sample}}{(TI_1)_{HSC}} \tag{6}$$

$$R_{TI_3} = \frac{(TI_3)_{sample}}{(TI_3)_{HSC}} \tag{7}$$

$$R_{TI_5} = \frac{(TI_5)_{sample}}{(TI_5)_{HSC}} \tag{8}$$

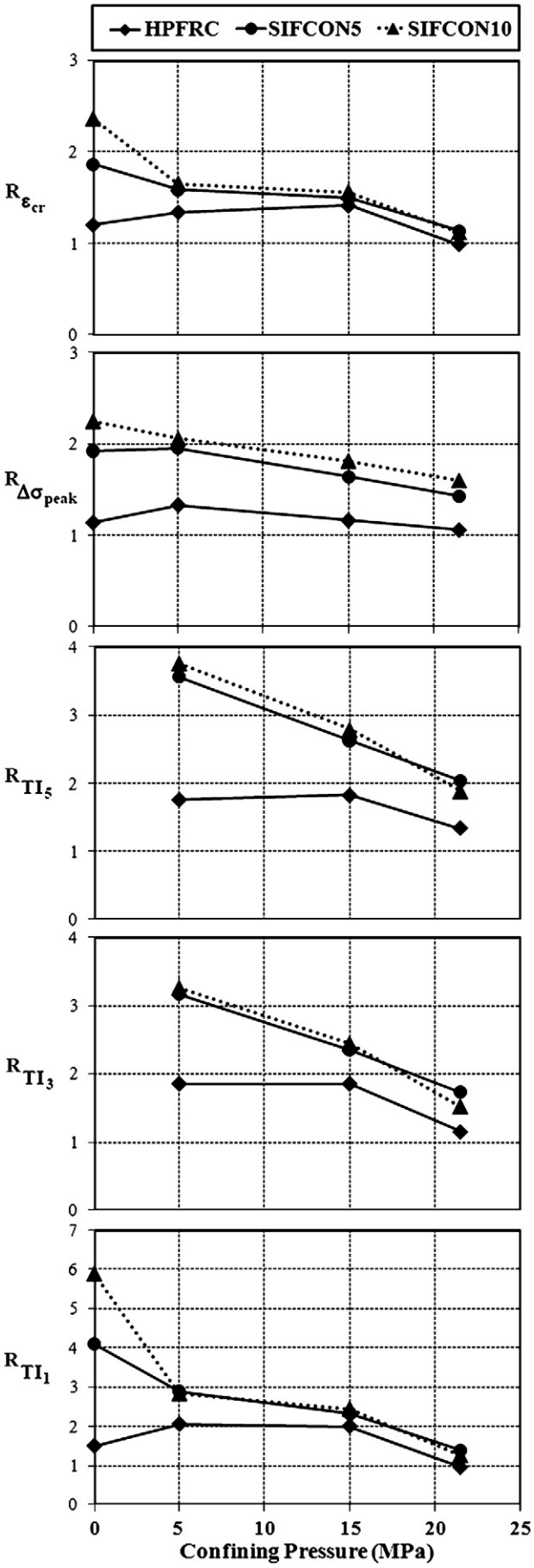

Fig. 17. Interrelated effects of fibre volume fraction and confining pressure.

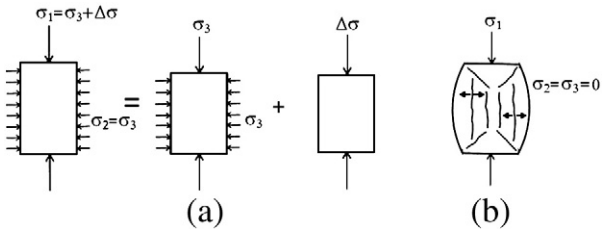

Fig. 18. (a) Linear superposition subjected to triaxial compression; (b) mode of specimen's failure subjected to uniaxial compression.

$$R_{\Delta\sigma_{peak}} = \frac{(\Delta\sigma_p)_{sample}}{(\Delta\sigma_p)_{HSC}} \tag{9}$$

$$R_{\varepsilon_{cr}} = \frac{(\varepsilon_{cr})_{sample}}{(\varepsilon_{cr})_{HSC}} \tag{10}$$

where $(TI_1)_{sample}$, $(TI_3)_{sample}$ and $(TI_5)_{sample}$ are TI_1, TI_3, TI_5 of HPFRC, SIFCON5 and SIFCON10 samples and also$(\Delta\sigma_p)_{sample}$ and $(\varepsilon_{cr})_{sample}$ are peak additional axial stress and first-crack strain of the samples, respectively. Similarly, $(TI_1)_{HSC}$, $(TI_3)_{HSC}$, $(TI_5)_{HSC}$, $(\Delta\sigma_p)_{HSC}$ and $(\varepsilon_{cr})_{HSC}$ have the same definitions but for HSC samples under corresponding confining pressure. The variations of these ratios under different confining pressures are indicated in Fig. 17.

As shown in Fig. 17, interrelated ratios decrease by increasing confining pressure for SIFCONs specimens. However, for HPFRC samples, some enhancement is observed especially under confining pressures ranging between 0 and 15 MPa and then this effect decreases. As a result, fibres play a less significant role on triaxial properties with increasing confining pressure. Furthermore, it is obvious that in triaxial conditions, increasing fibre content from 2% to 5% has more considerable effect than from 5% to 10%. On the other hand, in triaxial conditions, increasing fibre content up to 5% has a positive effect on enhancing specimens' properties but adding more fibres has a very limited additional effect.

4.5. Failure pattern

Steel fibre reinforced concrete (SFRC), especially SFRC with high volume fraction of fibre like SIFCON, under triaxial condition behaves quite differently compared to what is usually observed in plain concrete. The most important differences are hardening behaviour, higher multiaxial strength and ductility.

Based on the linear superposition of stress states shown in Fig. 18a, specimens should fail in a mode similar to uniaxial compression test (tensile failure), shown in Fig. 18b. However, it seems that lateral confinement pressures and adding steel fibres prevent the occurrence of cracks parallel to the direction of force, and causes the sample to fail differently and mainly in shear and crushing modes observed in tested specimens. Therefore, in triaxial loading, combining the effectiveness of fibres and confining pressure change the mode of failure for specimens.

Failure patterns of HSC, HPFRC, SIFCON5, and SIFCON10 specimens under triaxial compression are shown in Fig. 19. Since the failure modes were approximately similar in all the confining pressure ranges, the pictures for 5 MPa pressure test are depicted in Fig. 19.

For HSC samples, shear failure was observed on a very sharp diagonal plane which is typical of the brittle materials (Fig. 19a). For HPFRC specimens, adding 2% volume fraction of steel fibres into samples causes shear plane angle to decrease, but still a distinguished shear plane form. These samples also show other multiple shear cracks during loading, which is typical of a semi ductile material behaviour (Fig. 19b).

For SIFCON10, due to high volume of steel fibres, the tensile and shear strengths have increased since the failure mechanism is

Fig. 19. Failure Patterns of specimens under triaxial compression for (a) HSC; (b) HPFRC; (c) SIFCON5 and (d) SIFCON10.

crushing rather than shearing. Ductility accompanied with the high strength properties makes SIFCON a unique material which is suitable for a large variety of applications (Fig. 19d). SIFCON5 behaves as an intermediate material and shows some shearing and crushing behaviours as observed in HPFRC and SIFCON10 (Fig. 19c). In addition, for both types of SIFCON, the crushing failure was observed on the upper side of the sample while casting the mould. This occurs due to the gravity effect which causes higher fibre concentration at the bottom of the sample. This mechanism was not observed in HPFRC because of lower proportion of fibre and lacking vibration during the sample preparation.

4.6. Failure criteria

Two most applied failure criterions are used to calibrate the models with triaxial compression test results of HSC, HPFRC and SIFCONs, as described in the following.

4.6.1. Mohr-Coulomb failure criterion

The Mohr-Coulomb failure criterion model [26] is one of the pressure-dependent failure criteria that the pure shear (τ_{oct} or octahedral shear) depends linearly on the hydrostatic stress (σ_{oct} or octahedral normal stress). This model is the most applied classical model for explaining of failure envelope and is still used extensively due to its simplicity and relatively good accuracy. This failure surface should passes through the point of uniaxial compression exactly. The normalized form of Mohr-Coulomb can be expressed as:

$$\left(\frac{\sigma_1}{f_c'}\right) = 1 + k\left(\frac{\sigma_3}{f_c'}\right) \tag{11}$$

where ϕ represents the internal-friction angle of concrete, $\frac{k = 1 + \sin(\varphi)}{1 - \sin(\varphi)}$, and $\sigma_3 < \sigma_1$. Xie et al. [11] obtained k values between 4.47 and 5.10 for different kinds of HSC with uniaxal compressive strength upper than 67 MPa. Moreover, Lu and Hsu [17] obtained 4.0 and 3.95 as k value of HSC and SFHSC samples respectively. Based on the data presented by Ansari and Li [14,15], the k values for HSC samples are in range of 2.6 to 3.1. The main reason of their low values of k might be due to the high amounts of confining pressure ($\sigma_3 \cong 84\,MPa$, $f_c' = 84\,MPa$) which leads the linear behaviour of Mohr-Columb failure criteria in low confining pressure ratio to change to a non-linear one at higher confining pressure ratio. Candappa et al. [18] reported 5.3 as the k value for HSC. Based on the results of this research as shown in Fig. 20, the k values for HSC, HPFRC, SIFCON5 and SIFCON10 are respectively 4.46, 4.82, 4.82 and 4.37, and the internal-friction angle ϕ of specimens can be adopted as 39° to 41°. The values of k extracted from experimental results are in good agreement with those obtained from literature. It is observed that the k values and the internal-friction angle vary insignificantly with the change of steel fibre volume fraction.

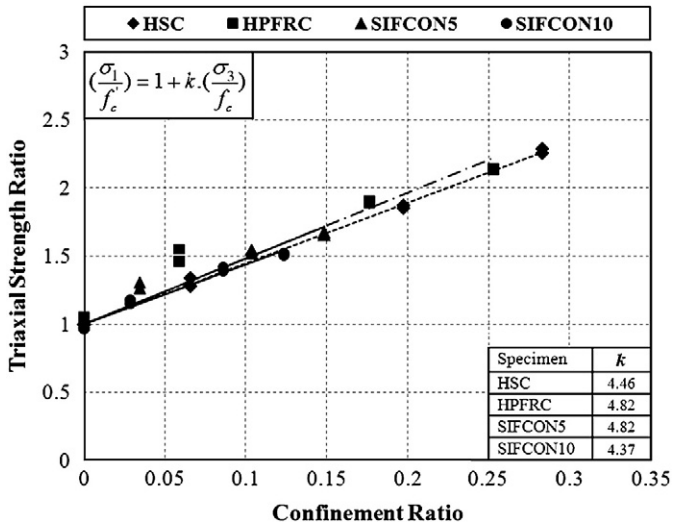

Fig. 20. Triaxial strength ratio versus confinement pressure ratio (Mohr-Coulomb failure criterion).

4.6.2. Willam-Warnke failure criterion

The Willam-Warnke is a five-parameter model which is widely used for FRC [10,17,27]. The Willam-Warnke model has curved compressive meridians expressed by quadratic parabolas of the form of

$$\frac{\tau_m}{f_c'} = c_0 + c_1\left(\frac{\sigma_m}{f_c'}\right) + c_2\left(\frac{\sigma_m}{f_c'}\right)^2 \quad (12)$$

where $\sigma_m = \frac{I_1}{3} = \frac{1}{3}(\sigma_1 + \sigma_2 + \sigma_3)$ and $\tau_m = \frac{1}{\sqrt{15}}\left[(\sigma_1-\sigma_2)^2 + (\sigma_2-\sigma_3)^2 + (\sigma_3-\sigma_1)^2\right]^{1/2}$ in which σ_m is mean normal stress, τ_m is mean shear stress, σ_1, σ_2 and σ_3 are the stresses in the three principal directions, and C_1, C_2 and C_3 are the Willam-Warnke model coefficients. Fig. 21 shows the variation of mean shear stress ratio versus mean normal stress ratio. Table 7 compares the model coefficients of HSC, HPFRC and SIFCONs with existing results in the literature. In Eq. (12), the C_2 coefficient shows the curve convexity of the results. For HSC, the C_2 is approximately zero and consequently τ_m is a linear function of σ_m. However, for HPFRC, SIFCON5 and SIFCON10 the coefficients show that the specimens behave with a similar non-linear and parabolic relationship under triaxial compression and τ_m is a parabolic function of σ_m. This difference exists probably due to the use of fibre in HPFRC and SIFCONs which greatly affects the behaviour of the concrete. The same behaviour was previously reported in the literature as shown in Table 7.

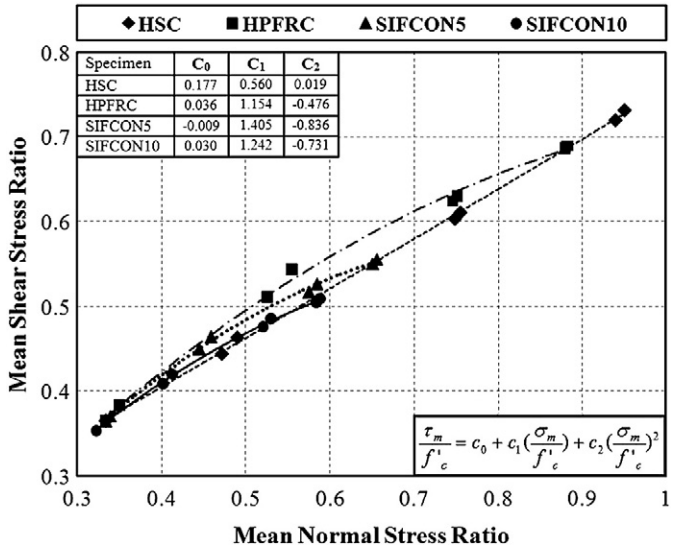

Fig. 21. Mean shear stress ratio versus mean normal stress ratio (Willam-Warnke failure criterion).

Table 7
Empirical coefficients for Willam-Warnke model.

Specimen	Uniaxial compression strength (MPa)	Max. of $\left(\frac{\sigma_3}{f_c'}\right)$	Max. of $\left(\frac{\sigma_1}{f_c'}\right)$	C_0	C_1	C_2
HSC	76	0.28	2.3	0.177	0.560	0.019
HPFRC	87	0.25	2.1	0.036	1.154	-0.476
SIFCON5	146	0.15	1.6	-0.009	1.405	-0.836
SIFCON10	171	0.13	1.5	0.030	1.242	-0.731
Ansari and Li [14]	47	0.9	3.5	0.157	0.668	-0.120
	71	0.9	3.2	0.141	0.753	-0.208
	107	0.8	2.9	0.149	0.721	-0.196
Li and Ansari [15]	70	1.0	3.4	0.155	0.726	-0.187
	103	0.8	3.2	0.108	0.870	-0.255
Lu and Hsu [17]	67	0.8	4.1	0.164	0.638	-0.054
	69	1.0	4.7	0.160	0.653	-0.055
Xie et al. [11]	60	0.5	3.2	0.126	0.771	-0.109
	92	0.5	3.2	0.088	0.902	-0.187
	119	0.5	3.1	0.075	0.921	-0.220
	42	0.3	2.5	0.120	0.769	-0.099
Candappa et al. [18]	61	0.2	1.9	0.162	0.610	-0.013
	73	0.2	1.9	0.053	1.062	-0.384
	103	0.1	1.6	0.035	1.162	-0.519

5. Conclusions

In this paper, the stress-strain responses of HSC, HPFRC and two types of SIFCON with 0, 2, 5 and 10% volume fraction of steel fibres subjected to triaxial compression have been investigated via a comprehensive experimental program. From the experimental results and related studies the following conclusions can be drawn:

- The triaxial mechanical properties of SFRC directly depend on two significant parameters including the steel fibre volume and confining pressure. Increase of volume fraction of steel fibres and confining pressure leads to ductile behaviour in SFRC and consequently its softening behaviour changes to plastic and hardening behaviour.
- Adding steel fibre up to 5% volume fraction has a considerable effect on triaxial mechanical properties of SFRC, while its effect is less in upper values.
- Increasing confining pressure and steel fibres volume increases the peak triaxial compressive strength. Also, adding steel fibres increases the Poisson's ratio for high strength concrete particularly for SIFCON with 10% volume fraction of steel fibres.
- Both confining pressure and fibre content have good effect on the toughness indices and they can raise the toughness of HSC up to 78 times.
- Study of interrelated effects of fibre volume fraction and confining pressure and also corresponding ratios shows that fibres play a less significant role on triaxial properties with increasing confining pressure.
- Shear failure occurred for HSC and HPFRC; whereas a combination of shear and crushing mode of failure was observed for SIFCON with 5% steel fibres. For SIFCON with 10% of steel fibre, only crushing mode of failure was observed.
- SIFCONs have unique triaxial compression characteristics such as high ductility, high triaxial compressive strength and hardening behaviour.
- Calibrated Mohr-Coulomb failure criterion for experimental data shows that adding steel fibres has insignificant effect on related coefficients whereas Willam-Warnke failure criterion is sensitive to increasing steel fibres volume fraction. This conclusion can be drawn for low confinement ratios and further tests should be

carried out to study concrete with high volume fraction of steel fibres under high confinement ratios.

References

[1] J. Gao, W. Sun, K. Morino, Mechanical properties of steel fibre-reinforced high-strength lightweight concrete, Cem. Concr. Compos. 19 (4) (1997) 307–313.
[2] M.C. Nataraja, N. Dhang, A.P. Gupta, Toughness characterization of steel fibre-reinforced concrete by JSCE approach, Cem. Concr. Res. 30 (4) (2000) 593–597.
[3] M.C. Nataraja, N. Dhang, A.P. Gupta, Stress–strain curves for steel-fibre reinforced concrete under compression, Cem. Concr. Compos. 21 (5–6) (1999) 383–390.
[4] P.S. Song, S. Hwang, Mechanical properties of high-strength steel fibre-reinforced concrete, Constr. Build. Mater. 18 (9) (2004) 669–673.
[5] Z. Hajar, D. Lecointre, A. Simon, J. Petitjean, Design and construction of the world first Ultra-High Performance Concrete road bridges, in: M. Schmidt, E. Fehling, C. Geisenhanslüke (Eds.), Proceedings of the International Symposium on Ultra High Performance Concrete, Kassel University Press, Kassel (Germany), 2004, pp. 39–48.
[6] A. Yan, K. Wu, X. Zhang, A quantitative study on the surface crack pattern of concrete with high content of steel fibre, Cem. Concr. Res. 32 (9) (2002) 1371–1375.
[7] A.E. Naaman, J.R. Homrich, Tensile stress-strain properties of SIFCON, ACI Mater. J. 86 (3) (1989) 244–251.
[8] A.E. Naaman, D. Otter, H. Najm, Elastic modulus of SIFCON in tension and compression, ACI Mater. J. 88 (6) (1992) 540–548.
[9] J. Linhua, H. Dahai, X. Nianxiang, Behavior of concrete under triaxial Compressive-Compressive-Tensile Stresses, ACI Mater. J. 88 (2) (1991) 181–185.
[10] J.C. Chern, H.J. Yang, H.W. Chen, Behaviour of steel fibre reinforced concrete in multiaxial loading, ACI Mater. J. 89 (1) (1992) 32–40.
[11] J. Xie, A.E. Elwi, J.G. MacGregor, Mechanical properties of three high-strength concretes containing silica fume, ACI Mater. J. 92 (2) (1995) 1–11.
[12] M.M. Attard, S. Setunge, Stress-strain relationship of confined and unconfined concrete, ACI Mater. J. 93 (5) (1996) 1–11.
[13] I. Imran, S.J. Pantazopoulou, Experimental study of plain concrete under triaxial stress, ACI Mater. J. 93 (6) (1996) 589–601.
[14] F. Ansari, Q. Li, High-strength concrete subjected to triaxial compression, ACI Mater. J. 95 (6) (1998) 747–755.
[15] Q. Li, F. Ansari, High-strength concrete in triaxial compression by different sizes of specimens, ACI Mater. J. 97 (6) (2000) 684–689.
[16] A. Mahboubi, A. Ajorloo, Experimental study of the mechanical behaviour of plastic concrete in triaxial compression, Cem. Concr. Res. 35 (2) (2005) 412–419.
[17] X. Lu, C.T.T. Hsu, Behavior of high strength concrete with and without steel fibre reinforcement in triaxial compression, Cem. Concr. Res. 36 (9) (2006) 1679–1685.
[18] D.C. Candappa, J.G. Sanjayan, S. Setunge, Complete triaxial stress strain curves of high-strength concrete, J. Mater. Civ. Eng. 13 (3) (2001) 209–215.
[19] Z.C. Girgin, N. Anoglu, E. Anoglu, Evaluation of strength criteria for very-high-strength concretes under triaxial compression, ACI Mater. J. 104 (3) (2007) 278–284.
[20] Y. Farnam, M. Shekarchi, A. Mirdamadi, Experimental investigation of impact behavior of high strength fiber reinforced concrete panels, in: E. Fehling, M. Schmidt, S. Sturwald (Eds.), Proceedings of the 2nd International Symposium on Ultra-High Performance Concrete, Kassel University Press, Kassel (Germany), 2008, pp. 751–758.
[21] ASTM C 801, Standard Test Method for Determining the Mechanical Properties of Hardened Concrete under Triaxial Loads, Annual book of ASTM Standards, American Society for Testing Materials, West Conshohocken, PA, 2005.
[22] E. Hoek, E.T. Brown, Underground excavations in rock, Institution of Mining and Metallurgy Press, London, 1980.
[23] D.A. Fanella, A.E. Naaman, Stress-strain properties of fiber reinforced mortar in compression, ACI J. 82 (4) (1985) 475–483.
[24] C.S. Poon, Z.H. Shui, L. Lam, Compressive behaviour of fibre reinforced high-performance concretre subjected to elevated temperatures, Cem. Concr. Res. 34 (12) (2004) 2215–2222.
[25] ASTM C 1018, Standard Test Method for Flexural Toughness and First-Crack Strength of Fiber-Reinforced Concrete (Using Beam with Third-Point Loading), Annual book of ASTM Standards, American Society for Testing Materials, West Conshohocken, PA, 2005.
[26] W.F. Chen, D.J. Han, Plasticity for structural engineers, Springer-Verlag Publication, New York, 1988.
[27] W.F. Chen, Plasticity in reinforced concrete, McGraw-Hill Publication, New York, 1982.